Statistics of the subgap states of $s_{\pm}$ superconductors

A. Glatz and A. E. Koshelev
Materials Science Division, Argonne National Laboratory, Argonne, Illinois 60439, USA
(Received 8 June 2010; published 21 July 2010)

There is strong support in favor of an unusual $s_{\pm}$ superconducting state in the recently discovered iron-based superconductors in which the gap parameter has opposite signs in different bands. In this case, scattering between different bands by impurities has a pair-breaking effect and introduces states inside the gap. We studied the statistics of disorder-induced subgap states in $s_{\pm}$ superconductors due to collective effects of impurities. Numerically solving the two-band Bogolyubov equations, we explored the behavior of the density of states and localization length. We located the mobility edge separating the localized and delocalized states for the three-dimensional case and the crossover between the weak and strong localization regimes for the two-dimensional case. We found that the widely used self-consistent T-matrix approximation is not very accurate in describing subgap states.

DOI: 10.1103/PhysRevB.82.012507 PACS number(s): 74.20.−z, 74.62.En, 74.70.Xa

The recent discovery of high-temperature superconductivity in the iron arsenide $LaFeAsO_{1-x}F_x$ (Ref. 1) followed by the discovery of several classes of superconducting materials[2] led to a major breakthrough in the field of superconductivity. The Fermi surface of these materials is composed of several electron and hole sheets located near different points of the Brillouin zone,[3] see Fig. 1(a). There is theoretical reasoning in favor of an electronic origin of superconductivity and a unusual superconducting state in which the order parameter has opposite signs in different bands ($s_{\pm}$ state).[4] This scenario is supported by the observation of a resonant magnetic mode in the superconducting state by inelastic neutron scattering.[5] Establishing the nature and mechanism of superconductivity in iron pnictides became one of the most urgent current problems in condensed-matter physics.

In the $s_{\pm}$ state, interband scattering due to potential impurities [see Fig. 1(a)] has a pair-breaking effect similar to magnetic impurities in conventional superconductors.[6,7] Such impurities introduce states inside the gap known as Shiba-Rusinov states for the magnetic-impurities problem.[7,8] This leads to a finite density of states (DoS) at zero energy and strongly influences the superconducting properties at low temperatures. Most iron pnictides are doped superconductors and disorder due to dopant atoms is unavoidable. Scattering effects are expected to be especially strong in Fe-substituted materials, such as Co- and Ni-doped 122 compounds. Experimental properties of iron pnictides which may be explained by a finite DoS at the Fermi level due to pair-breaking disorder include the "residual" linear temperature (T) dependence of the specific heat in the superconducting state[9] and a T^2 dependence of the London penetration depth at low temperatures.[10]

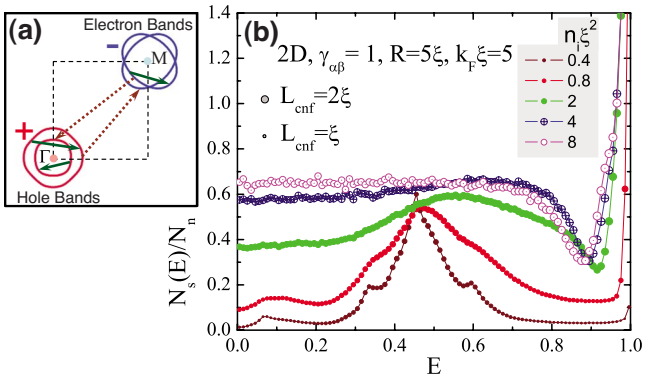

FIG. 1. (Color online) (a) The schematic band structure of iron pnictides. Solid and dotted arrows illustrate intraband and interband scattering events. (b) Evolution of the 2D subgap DoS with increasing concentration of impurities n_i for isotropic scattering. Symbol sizes are proportional to L_{cnf} [Eq. (3)]. E is given in units of Δ.

Transport properties at low temperatures, such as thermal conductivity[11,12] and microwave surface resistance, are sensitive to the localization state of the low-energy quasiparticles. A random impurity potential may localize quasiparticles within some energy range. For three-dimensional (3D) superconductors with moderately strong scatterers, we expect two regimes: (i) at small concentrations of impurities, states at the Fermi level are localized and a mobility edge at a finite energy exists, similar to the impurity bands in semiconductors; (ii) at sufficiently high impurity concentrations, all states are delocalized. The critical impurity concentration depends on the scattering properties of the impurities. In the first regime, localized states near zero energy contribute to the low-temperature behavior of the thermodynamic but not transport properties. The quantity of interest is the zero-energy DoS at a critical impurity concentration. One of the consequences of *delocalized* states at the Fermi level is a linear temperature term in the thermal conductivity. The existence of such term in the iron pnictides is a controversial issue, for example, a large linear term in the thermal conductivity was reported for the compound $Ba[Fe_{1-x}Co_x]_2As_2$ in Ref. 11 but no linear term at zero magnetic field was found for the same compound in Ref. 12, even though the same group reported a T^2 behavior of the London penetration depth. This probably indicates that the localization state of quasiparticles is very sensitive to the disorder level of the samples. Even though, on general grounds, both situations are possible, proper interpretation of these experiments is impossible without the development of a quantitative theory of quasiparticle localization due to the pair-breaking scattering.

A standard analytical approach to describe collective effects of impurities in superconductors is the self-consistent T-matrix (SCTM) approximation. For the Born limit, it was elaborated in the famous paper by Abrikosov and Gor'kov[6] and was later generalized for strong scattering.[7] Most theoretical works on collective effects of impurities in superconductors are based on this approximation, see, e.g., the review.[8] While giving a qualitative description of the impurity band, the SCTM approximation has serious deficiencies. For small impurity concentrations, it predicts a hard gap in the spectrum. In reality, the DoS is finite at all energies, it has an exponential tail[13] due to rare fluctuation configurations of impurities, similar to the Lifshitz tail in the impurity band of semiconductors. Another deficiency of the SCTM description is that it ignores localization properties of the states. Localization of quasiparticles in superconductors was studied for dirty d-wave superconductors[14] and for the mixed state of disordered s-wave superconductors.[15] To our knowledge, localization in the impurity band of superconductors with pair-breaking impurities was never studied.

A general treatment of nonmagnetic impurities in multiband superconductors has been developed in several early papers.[16] Several recent papers address different aspects of the impurity-induced subgap states[17,18] and their possible influence on properties of iron pnictides.[19] Studies of collective impurity effects, however, do not go beyond the SCTM approach. Motivated by the importance of disorder-induced subgap states for the properties of iron pnictides and the absence of an accurate theoretical description of these states, we performed a detailed study of their statistical properties based on numerical calculations. We explore the behavior of the density of states for $s_{\pm}$ superconductors as a function of scattering parameters and impurity concentration and compare the results with the SCTM approach. We also explore localization properties of states in order to locate the mobility edge in the parameter space.

We use the simplest model of a disordered $s_{\pm}$ superconductor, which is described by the two-band Bogolyubov equations for the two-component wave functions, $\hat{\Psi}_{\alpha}=\binom{u_{\alpha}}{v_{\alpha}}$,

$$(E-\hat{\varepsilon}_{\alpha}\hat{\tau}_z+\Delta_{\alpha}\hat{\tau}_x)\hat{\Psi}_{\alpha}(\mathbf{r})-\hat{\tau}_z\sum_{l,\beta}\delta(\mathbf{r}-\mathbf{R}_l)U^l_{\alpha\beta}\hat{\Psi}_{\beta}(\mathbf{r})=0.$$

Here α is the band index, $\hat{\tau}_i$ are Pauli matrices in Nambu space, $\hat{\varepsilon}_{\alpha}=\xi_{\alpha}(\hat{\mathbf{k}})-\varepsilon_F\approx\mathbf{v}_{F,\alpha}(\hat{\mathbf{k}}-\mathbf{k}_{F,\alpha})$, and Δ_{α} are the gap parameters. We assume that $\Delta_2=-\Delta_1$. The last term in the equation describes the interaction with impurities. The interband scattering is described by the off-diagonal terms in the matrix $U^l_{\alpha\beta}$. For scattering between bands 1 and 2, separated by wave vector $\mathbf{Q}$ equal to half of the reciprocal-lattice vector, U^l_{12} contains the factor $\exp(i\mathbf{Q}R_l)$ which only takes values ±1 depending on $\mathbf{R}_l$. This means that even for identical impurities U^l_{12} has random signs and its average is zero. We neglect inhomogeneities of the gap parameters due to impurities. It is known that these inhomogeneities are small and do not influence the quasiparticle states much. The key parameter of an isolated pair-breaking impurity is the energy of a localized state,[18] $E_0/\Delta\equiv\varepsilon_0=\sqrt{1-4\Gamma_{\mathrm{eff}}}$, where we introduced the effective interband scattering parameter,

$$\Gamma_{\mathrm{eff}}=\frac{\gamma_{12}\gamma_{21}}{1+\gamma_{22}^2+\gamma_{11}^2+2\gamma_{12}\gamma_{21}+(\gamma_{22}\gamma_{11}-\gamma_{12}\gamma_{21})^2} \quad (1)$$

with $\gamma_{\alpha\beta}=\pi\nu_{\alpha}U_{\alpha\beta}$ being the reduced scattering amplitudes and $\nu_{\alpha}=\int\frac{d^d\mathbf{k}}{(2\pi)^d}\delta[\xi_{\alpha}(\mathbf{k})-\varepsilon_F]$ being the normal DoS (per spin) for band α.

We explore the properties of the subgap states for the two- and three-dimensional cases. For the numerical analysis, we rewrite the equations in a form containing only wave functions at the impurity sites,

$$\hat{\Psi}_{\alpha}(\mathbf{R}_l)=\sum_{\beta,l'}\hat{g}_{\alpha}(\mathbf{R}_l-\mathbf{R}_{l'})\hat{\tau}_z\gamma'_{\alpha\beta}\hat{\Psi}_{\beta}(\mathbf{R}_{l'}), \quad (2)$$

where the reduced Green's function is defined as

$$\hat{g}_{\alpha}(\mathbf{R})=\frac{1}{\pi\nu_{\alpha}}\int\frac{d^d\mathbf{k}}{(2\pi)^d}\exp(i\mathbf{k}\mathbf{R})\frac{E+\varepsilon_{\alpha}(\mathbf{k})\hat{\tau}_z-\Delta_{\alpha}\hat{\tau}_x}{E^2-\varepsilon^2_{\alpha}(\mathbf{k})-\Delta^2_{\alpha}}$$

and d is the spatial dimensionality. For each impurity realization inside a box of size R^d, we find the set of eigenenergies E_{λ} and the corresponding four-component wave functions $\hat{\Psi}^{\lambda}_l=[\hat{\Psi}^{\lambda}_1(\mathbf{R}_l),\hat{\Psi}^{\lambda}_2(\mathbf{R}_l)]$, see supplementary materials.[20] From the set of eigenenergies, we compute the average DoS, $N_s(E)=\langle\Sigma_{\lambda}\delta(E-E_{\lambda})\rangle$, where the average is taken over many impurity realizations. We normalize $N_s(E)$ to the total normal DoS for excitations, $N_n=4\nu$. To characterize localization properties, we compute the average confinement length for given energy,

$$L_{\mathrm{cnf}}(E,R)=\left\langle\sqrt{\sum_{a=x,y[,z]}(\langle r_a^2\rangle_{\lambda}-\langle r_a\rangle^2_{\lambda})}\right\rangle_{E_{\lambda}=E}, \quad (3)$$

where $\langle r_a^m\rangle_{\lambda}=\Sigma_l R^m_{l,a}|\Psi^{\lambda}_l|^2$ $(m=1,2)$ and $|\Psi^{\lambda}_l|^2=\Sigma_{\alpha}[|u^{\lambda}_{\alpha}(\mathbf{R}_l)|^2+|v^{\lambda}_{\alpha}(\mathbf{R}_l)|^2]$. The behavior of $L_{\mathrm{cnf}}(E,R)$ with increasing system size, R, determines the nature of the states. For delocalized states, $L_{\mathrm{cnf}}(E,R)$ is limited by the system size and linearly grows with R. For localized states, $L_{\mathrm{cnf}}(E,R)$ saturates at a finite value, which gives the average localization length of states with energy E, $\lim_{R\to\infty}L_{\mathrm{cnf}}(E,R)=L_{\mathrm{loc}}(E)$.

We study the subgap densities of states at different concentrations of impurities and scattering parameters. We consider the case of isotropic scattering, when all matrix elements $\gamma_{\alpha\beta}$ are equal. Figure 1(b) shows the evolution of the subgap DoS with increasing concentration of impurities n_i for a moderate scattering rate, $\gamma_{\alpha\beta}=1$ for all α and β, and the system size $R=5\xi$. The energy is normalized to the gap value Δ and the coherence length is defined as $\xi=v_F/\Delta$. For small concentrations of impurities, the DoS has a peak near the energy of the localized state. With increasing impurity concentrations, the peak broadens and becomes completely smeared already at relatively small impurity concentration $n_i\xi^2=2$. At higher concentrations, the DoS becomes almost constant and comparable with the normal DoS. The left part of Fig. 2 shows the subgap DoS for two impurity concentrations for a wide range of isotropic scattering rates. The energy location of the peak for small concentrations goes down with increasing scattering strength while the maximum DoS is almost independent of $\gamma_{\alpha\beta}$. The peak smears with increasing impurity concentration and the magnitude of the density

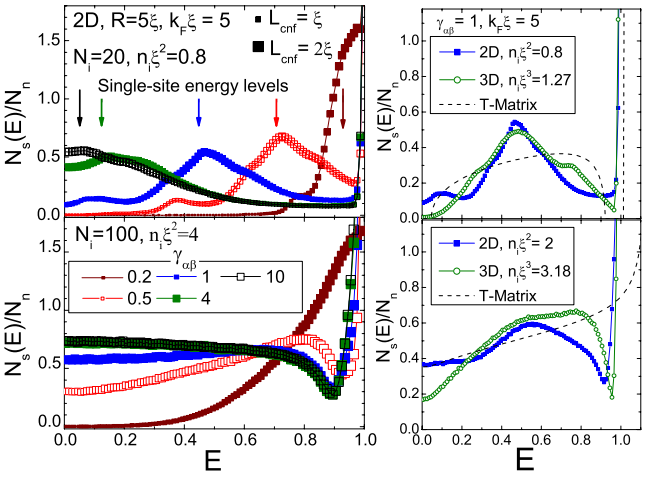

FIG. 2. (Color online) Left: evolution of the subgap DoS with changing scattering rate for isotropic scattering for two impurity concentrations (unit of E is Δ). Symbol sizes are proportional to the confinement length. Right: comparison of the DoS shapes for the 2D and 3D models with identical pair-breaking parameters and SCTM results for two impurity concentrations.

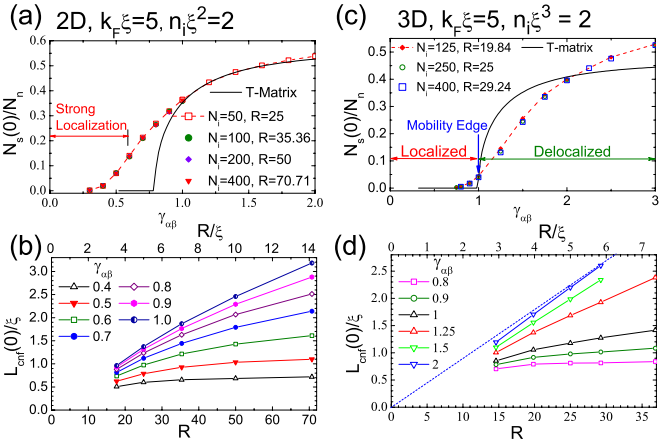

FIG. 3. (Color online) Plots (a) and (c) show the dependences of the zero-energy DoS on the scattering strength for isotropic scattering for 2D and 3D cases. Solid lines show the SCTM results. Plots (b) and (d) show the size dependences of the confinement length at different scattering strength (lengths are in units of k_F^{-1}).

of states at large concentrations depends only weakly on the scattering strength for $\gamma_{\alpha\beta}>0.5$. Also, for large scattering rates, the DoS approaches a limiting shape corresponding to the unitary limit. For small scattering strength, $\gamma_{\alpha\beta}=0.2$, we found the typical "Lifshitz tail" behavior.

Within the SCTM approximation,[20] the DoS does not depend on dimensionality of superconductor, it is determined by the location of the single-site energy level and the pair-breaking parameter proportional to the impurity concentration $\alpha=2n_i\Gamma_{\text{eff}}/(\pi\nu\Delta)$. Even though the overall evolution of the DoS shape with variations in the scattering strength and impurity concentration is similar in the 2D and 3D cases, the universality suggested by the SCTM approach does not exist. In the right part of Fig. 2, we compare the computed DoS for two impurity concentrations corresponding to the same pair-breaking strength in the 2D and 3D cases with the SCTM results. One can see that the DoS shapes for the two dimensionalities are similar but not identical. One noticeable difference is that the 3D DoS is typically smaller at low energies. The SCTM approximation does not reproduce the DoS shape at low impurity concentrations, the sharp peak in the center and the small features at the sides are not reproduced. These features appear due to the oscillating dependence of the impurity-pair energy on their separation and correspond to the impurity pairs separated by the distances at which these energies have extrema.[20] For large impurity concentration, we found a dip in the DoS for energies slightly smaller than Δ, also not reproduced by the SCTM approximation.

We now focus on the region near zero energy, which determines the low-temperature behavior of the superconducting parameters. Figures 3(a) and 3(c) show the dependences of the zero-energy DoS on the isotropic scattering strength for fixed impurity concentration for the 2D and 3D models. We see that the DoS has a negligible size effect even at the smallest studied sizes. The SCTM approximation only roughly reproduces the shape of the numerical curves and does not describe the tail region. The size dependences of the confinement length are shown in Figs. 3(b) and 3(d). We can see that for the 2D case at $\gamma_{\alpha\beta}<0.6$, the confinement length saturates at large R approaching a finite localization length. No clear saturation of L_{cnf} is observed for $\gamma_{\alpha\beta}>0.6$. This may imply that states are delocalized or the localization length may be much larger than the studied system sizes. The second possibility looks more plausible because for 2D disordered systems, all electronic states are expected to be localized. The region $\gamma_{\alpha\beta}\approx 0.6$ probably marks a sharp crossover between the weak and strong localization regimes. We actually observe a noticeable downward curvature in the dependences of L_{cnf} vs R for all $\gamma_{\alpha\beta}$ which may be interpreted as a tendency toward localization at larger length scales. For the 3D case, we expect a true mobility edge which we can estimate as the value of $\gamma_{\alpha\beta}$ at which L_{cnf} has a clear saturation tendency at large R. The estimated location of the mobility edge, $\gamma_{\alpha\beta}\approx 1$, is marked in Fig. 3(c). It is close to the critical value bounding the SCTM gapped regions. We found that the DoS values at the mobility edge are quite small ($\sim$0.05 in our example). These values are significantly smaller than the DoS at the localization crossover for the 2D case. This observation implies that for identical bands in the 3D case, there is only a very narrow parameter window within which the localized states at zero energy provide a noticeable DoS.

The accumulation of states at the Fermi level with increasing impurity concentration is accompanied by a suppression of superconductivity. In Figs. 4(a) and 4(b), we compare the numerical and SCTM dependences of the zero-energy 2D DoS on the impurities concentration for weak and strong isotropic scattering. We also show the concentration dependences of the transition temperature evaluated using the Abrikosov-Gor'kov formula.[6,20] For small scattering strength, a noticeable DoS appears at the Fermi level only when T_c is strongly suppressed. In contrast, for large scattering strength, the DoS reaches values comparable with the normal DoS already at very minor suppression of T_c.

In conclusion, we explored the subgap DoS and localiza-

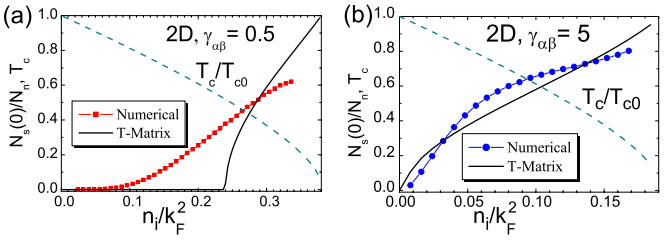

FIG. 4. (Color online) These plots show the dependences of the zero-energy 2D DoS and transition temperature on concentration of impurities for two isotropic scattering rates, (a) γ=0.5 and (b) γ =5. The clean-limit coherence length is taken as $k_F\xi$=2.63.

tion properties for disordered $s_{\pm}$ superconductors. We found that the widely used analytical description (SCTM) is incomplete and not very accurate. Disorder makes superconductivity "gapless," the DoS at E=0 is always finite. In the 3D case at low impurity concentrations, there is a mobility edge separating localized and delocalized states. In this regime, the localized states at the Fermi level contribute to low-temperature thermodynamic properties but do not contribute to transport. The mobility edge reaches zero energy at a critical impurity concentration above which all states become delocalized. In the 2D case, the mobility edge is replaced by a crossover separating strongly and weakly localized states. The development of quantitative theory of the subgap states is crucial for the understanding properties of the iron pnictides and other superconductors with pair-breaking impurities.

We would like to thank I. Vekhter, T. Proslier, K. Matveev, and U. Welp for useful discussions. This work is supported by UChicago Argonne, LLC, under Contract No. DE-AC02-06CH11357 and by the Center for Emergent Superconductivity, an Energy Frontier Research Center funded by the U.S. DOE, Office of Science, Office of BES under Award No. DE-AC0298CH1088.

[1] Y. Kamihara, T. Watanabe, M. Hirano, and H. Hosono, J. Am. Chem. Soc. **130**, 3296 (2008).

[2] C. W. Chu, F. Chen, M. Gooch, A. M. Guloy, B. Lorenz, B. Lv, K. Sasmal, Z. J. Tang, J. H. Tapp, and Y. Y. Xue, Physica C **469**, 326 (2009); D. Johrendt and R. Pöttgen, *ibid.* **469**, 332 (2009); M. K. Wu *et al.*, *ibid.* **469**, 340 (2009); A. S. Sefat, D. J. Singh, R. Jin, M. A. McGuire, B. C. Sales, F. Ronning, and D. Mandrus, *ibid.* **469**, 350 (2009); P. M. Shirage *et al.*, *ibid.* **469**, 355 (2009); J. Karpinski, *ibid.* **469**, 370 (2009); X. Zhu, F. Han, P. Cheng, G. Mu, B. Shen, B. Zeng, and H.-H. Wen, *ibid.* **469**, 381 (2009).

[3] D. J. Singh, Physica C **469**, 418 (2009); I. I. Mazin and J. Schmalian, *ibid.* **469**, 614 (2009).

[4] I. I. Mazin, D. J. Singh, M. D. Johannes, and M. H. Du, Phys. Rev. Lett. **101**, 057003 (2008); K. Kuroki, S. Onari, R. Arita, H. Usui, Y. Tanaka, H. Kontani, and H. Aoki, *ibid.* **101**, 087004 (2008).

[5] A. D. Christianson, E. A. Goremychkin, R. Osborn, S. Rosenkranz, M. D. Lumsden, C. D. Malliakas, I. S. Todorov, H. Claus, D. Y. Chung, M. G. Kanatzidis, R. I. Bewley, and T. Guidi, Nature (London) **456**, 930 (2008).

[6] A. A. Abrikosov and L. P. Gor'kov, Zh. Eksp. Teor. Fiz. **39**, 1781 (1960) [Sov. Phys. JETP **12**, 1243 (1961)].

[7] H. Shiba, Prog. Theor. Phys. **40**, 435 (1968); A. I. Rusinov, JETP Lett. **9**, 85 (1969); Sov. Phys. JETP **29**, 1101 (1969).

[8] A. V. Balatsky, I. Vekhter, and Jian-Xin Zhu, Rev. Mod. Phys. **78**, 373 (2006).

[9] J. K. Dong, L. Ding, H. Wang, X. F. Wang, T. Wu, G. Wu, X. H. Chen, and S. Y. Li, New J. Phys. **10**, 123031 (2008); M. Gang, Z. Bin, C. Peng, W. Zhao-Sheng, F. Lei, S. Bing, S. Lei, R. Cong, and W. Hai-Hu, Chin. Phys. Lett. **27**, 037402 (2010).

[10] C. Martin, R. T. Gordon, M. A. Tanatar, H. Kim, N. Ni, S. L. Bud'ko, P. C. Canfield, H. Luo, H. H. Wen, Z. Wang, A. B. Vorontsov, V. G. Kogan, and R. Prozorov, Phys. Rev. B **80**, 020501 (2009); R. T. Gordon, C. Martin, H. Kim, N. Ni, M. A. Tanatar, J. Schmalian, I. I. Mazin, S. L. Bud'ko, P. C. Canfield, and R. Prozorov, *ibid.* **79**, 100506 (2009); K. Hashimoto, T. Shibauchi, S. Kasahara, K. Ikada, S. Tonegawa, T. Kato, R. Okazaki, C. J. van der Beek, M. Konczykowski, H. Takeya, K. Hirata, T. Terashima, and Y. Matsuda, Phys. Rev. Lett. **102**, 207001 (2009).

[11] Y. Machida, K. Tomokuni, T. Isono, K. Izawa, Y. Nakajima, and T. Tamegai, J. Phys. Soc. Jpn. **78**, 073705 (2009).

[12] M. A. Tanatar, J.-Ph. Reid, H. Shakeripour, X. G. Luo, N. Doiron-Leyraud, N. Ni, S. L. Bud'ko, P. C. Canfield, R. Prozorov, and L. Taillefer, Phys. Rev. Lett. **104**, 067002 (2010).

[13] A. V. Balatsky and S. A. Trugman, Phys. Rev. Lett. **79**, 3767 (1997); A. Lamacraft and B. D. Simons, *ibid.* **85**, 4783 (2000); Phys. Rev. B **64**, 014514 (2001); A. V. Shytov, I. Vekhter, I. A. Gruzberg, and A. V. Balatsky, Phys. Rev. Lett. **90**, 147002 (2003).

[14] T. Senthil, M. P. A. Fisher, L. Balents, and C. Nayak, Phys. Rev. Lett. **81**, 4704 (1998); A. G. Yashenkin, W. A. Atkinson, I. V. Gornyi, P. J. Hirschfeld, and D. V. Khveshchenko, *ibid.* **86**, 5982 (2001).

[15] R. Bundschuh, C. Cassanello, D. Serban, and M. R. Zirnbauer, Phys. Rev. B **59**, 4382 (1999); S. Vishveshwara, T. Senthil, and M. P. A. Fisher, *ibid.* **61**, 6966 (2000).

[16] C. C. Sung and V. K. Wong, J. Phys. Chem. Solids **28**, 1933 (1967); G. Preosti and P. Muzikar, Phys. Rev. B **54**, 3489 (1996); A. A. Golubov and I. I. Mazin, *ibid.* **55**, 15146 (1997); M. L. Kulić and O. V. Dolgov, *ibid.* **60**, 13062 (1999).

[17] Y. Senga and H. Kontani, J. Phys. Soc. Jpn. **77**, 113710 (2008); New J. Phys. **11**, 035005 (2009).

[18] M. Matsumoto, M. Koga, and H. Kusunose, J. Phys. Soc. Jpn. **78**, 084718 (2009).

[19] A. B. Vorontsov, M. G. Vavilov, and A. V. Chubukov, Phys. Rev. B **79**, 140507(R) (2009); Y. Bang, EPL **86**, 47001 (2009).

[20] See supplementary material at http://link.aps.org/supplemental/10.1103/PhysRevB.82.012507 for (i) the SCTM approximation, (ii) the details of the simulation procedure, and (iii) the DoS shape at small concentrations dominated by impurity pairs.